



## CFD Analysis of Heat Exchanger Effectiveness and LMTD with Varying Pipe Length

Shahed A. Al-Rawashdeh <sup>1\*</sup>

<sup>1</sup> Department of Marine Science, Al Balqa Applied University, Aqaba, Jordan.

### Abstract

This paper presents a new numerical analysis for 2D heat exchanger (HE) model by employing computational fluid dynamics (CFD) simulations to analyze the impact of pipe length on the efficiency and the Log Mean Temperature Difference (LMTD) of parallel and counterflow double-pipe heat exchangers while maintaining constant flow rates, inlet temperatures, and fluid properties. The findings demonstrate that heat exchanger efficiency and LMTD in both the parallel and counterflow HEs are significantly influenced by pipe length, with longer heat exchangers improving heat transfer effectiveness by allowing more time for thermal exchange, larger heat exchange surface area, and achieving a more uniform temperature distribution. Counterflow heat exchangers also showed higher efficiencies at all lengths than parallel flow heat exchangers due to the larger temperature difference between the fluids. These insights are particularly valuable for engineers and designers seeking to optimize heat exchanger configurations for industrial applications, where enhancing heat transfer efficiency and minimizing energy losses are critical for cost-effective and sustainable thermal management systems.

### Keywords:

Heat Transfer;  
Heat Exchanger;  
Effectiveness;  
CFD; LMTD.

### Article History:

<b>Received:</b>	07	March	2025
<b>Revised:</b>	27	June	2025
<b>Accepted:</b>	05	July	2025
<b>Published:</b>	01	August	2025

## 1- Introduction

Environmental and energy issues are among the most important pressing challenges in the world, particularly in recent times [1-3]. Given the growing demand for energy across various sectors, ensuring the efficient use of available energy with minimal losses is critical [4, 5]. This highlights the need for high-efficiency energy transmission systems, such as heat exchangers (HEs), turbines, pumps, and other supporting components. HEs are considered one of the most important systems used for transferring heat energy in a variety of engineering applications, including power plants and automobile engines [6-10]. Here, work to optimize heat energy transport and recycle from heat exchangers is highlighted. An HE is a device or system that facilitates heat transfer between two or more media, which may be liquid, gaseous, or both [11, 12]. These media may be separated by a solid wall of a specific thickness to prevent mixing, or heat transfer may occur through direct contact between the media with no physical barriers or separators between them [13]. The operation of heat exchangers primarily depends on their design, the flow rate inside the HE, the nature of materials used in construction, and their thermal properties [9, 13-15].

HEs are typically made of copper, aluminum, carbon steel, stainless steel, and titanium alloys. However, aluminum and copper alloys are the two most commonly used materials for HEs. Both metals have excellent thermal properties and corrosion resistance, making them excellent choices [16]. The function of the HEs is determined and classified into several types based on their characteristics, such as process function (cooling or heating), fluid flow direction,

\* **CONTACT:** [shahed.rawashdeh.27@bau.edu.jo](mailto:shahed.rawashdeh.27@bau.edu.jo)

**DOI:** <http://dx.doi.org/10.28991/ESJ-2025-09-04-020>

© 2025 by the authors. Licensee ESJ, Italy. This is an open access article under the terms and conditions of the Creative Commons Attribution (CC-BY) license (<https://creativecommons.org/licenses/by/4.0/>).

construction (tubular, plate, regenerative, and extended surface), and heat transfer mechanisms [17-19]. Therefore, there are four types of HEs: concentric pipe heat exchangers, cross-flow heat exchangers, shell-and-tube heat exchangers, and compact heat exchangers. The most common type of HE is the concentric pipe or double pipe heat exchanger, in which one pipe is placed inside another due to its simplicity, reliability, and ease of maintenance [19, 20]. These HEs can be configured in two main ways: counterflow and parallel flow. The counterflow arrangement, where the fluids flow in opposite directions, generally provides higher heat transfer efficiency than the parallel flow configuration [21].

Double-pipe HEs are utilized to collect and recycle energy in various traditional or renewable energy systems [22, 23]. These devices are essential for completing engineering cycles, and certain systems cannot function properly without them. Therefore, the effectiveness of a heat exchanger and its heat transfer performance are critical considerations in the design of HE [23]. In double-pipe HE, the Log Mean Temperature Difference (LMTD) is a crucial parameter that affects heat transfer efficiency. LMTD represents the temperature variation between the hot and cold fluids at different points along the exchanger [24, 25]. The heat transfer efficiency and LMTD in these exchangers are significantly impacted by various factors such as the fluid flow dynamics, material of the pipes, properties of the fluids, and geometric factors like the diameter and length of the pipes [14, 24]. Hesselgreaves et al. [9] and Miguel & Rocha [26] highlighted that the LMTD approach is influenced by factors such as the length, diameter, and flow configuration of the heat exchanger. In particular, the geometric dimensions of the inner and outer pipes directly affect the heat transfer rate and pressure drop. A study by Kays and London focused on the relationship between LMTD and the flow arrangement, noting that countercurrent flow configurations generally result in higher heat transfer rates compared to parallel flow [27]. Additionally, experimental and numerical investigations, such as those by Zhang & Davie [28] have analyzed the effects of pipe diameter and length on the heat transfer coefficient and pressure drop in double-pipe HE. Moreover, studies by Mangrulkar et al. [29] demonstrated that increasing the length-to-diameter ratio of the pipe enhances the LMTD, which in turn increases the heat transfer rate.

The design of HEs plays a pivotal role in heat transfer, affecting the flow pattern, thermal boundary layer development, and available heat transfer area. Several studies have been conducted to explore how the geometry of two-pipe HEs can improve their performance [30, 31]. They examined how the design of heat exchangers affects both the rate of heat transfer and the distribution of temperature within the system. The findings showed that different design parameters—such as the shape, size, and arrangement of the exchanger—can significantly influence how efficiently heat is transferred. This research highlighted the importance of optimizing heat exchanger design to improve thermal performance and energy efficiency [30]. Ghaderi et al. [32] examined the effects of various geometrical modifications, including pipe diameter, spacing between the two pipes, and the effect of insulation thickness. Their study concluded that increasing the pipe diameter and optimizing the spacing between the pipes improved heat transfer by reducing the thermal resistance, especially under turbulent flow conditions. Ajay et al. [33] conducted a study comparing heat transfer performance in double-pipe HEs with varying geometrical configurations, including eccentric and concentric pipe arrangements. Their numerical results showed that eccentric arrangements of the inner and outer pipes provided better heat transfer rates due to the increased turbulence and mixing, whereas concentric designs were more suited for laminar flow conditions. Khaled et al. [34] have also looked into more advanced design modifications to enhance heat transfer while considering pipe length. Xie et al. [35] studied the effect of pipe length on heat transfer in HEs with enhanced surfaces (such as finned tubes). Their findings indicated that for HEs with enhanced surfaces, the effect of pipe length was more pronounced, as longer pipes allowed for a more significant improvement in heat transfer due to the increased surface area. However, the study emphasized that the optimal pipe length depended heavily on the type of enhancement and the flow regime. Zhao & Deng [36] explored the impact of pipe length on heat transfer performance in the presence of turbulent flow. They found that the optimal length for turbulent flow was shorter compared to laminar flow conditions, as the increased turbulence effectively enhanced the heat transfer coefficient over shorter distances, reducing the need for long pipes.

In recent years, numerical simulation has become increasingly crucial for optimizing the length of pipes in HEs, serving as a powerful tool to analyze heat transfer and fluid flow behaviors. Computational fluid dynamics (CFD) simulation provides valuable insights into temperature distribution, velocity patterns, and local heat transfer characteristics, enabling more accurate predictions of HE performance under various geometries through mathematical equations based on the law of conservation of energy, momentum, and mass [37-42]. It is a dynamic simulator that converts differential flow equations into integrated algebraic equations to produce approximate solutions that mimic practical and laboratory results [43-48]. Additionally, CFD is distinguished by its combination of mathematical and physical modeling of engineering phenomena, as well as the application of a variety of numerical methods to achieve highly accurate results and graphs in the shortest amount of time [48-54]. For instance, studies by Karwa [55] and Saha et al. [56] employed CFD simulations to investigate the impact of geometric variations, such as pipe length, diameter, and the flow configuration, on heat transfer performance. Meesala et al. [57] developed a 3D CFD model to study. They concluded that the temperature gradient, and consequently the LMTD, increased as the length of the pipes was extended. However, the computational cost of simulating longer pipes became prohibitive, suggesting the use of simplified models for longer HEs.

Despite the valuable insights provided by these studies, gaps remain in the comprehensive understanding of the combined effect of geometry and pipe length on the heat transfer performance of double-pipe HEs. Previous studies have focused primarily on isolated effects of geometry or flow arrangements, but few have integrated the effects of these parameters in a systematic manner to create more accurate performance models. This research aims to address this gap by employing numerical simulations to investigate the impact of the length of copper double-pipe HEs on the LMTD and, consequently, the heat transfer performance. This study will explore a range of pipe lengths (250, 550, 700, and 1000 mm) under constant operating conditions like flow rates, inlet temperatures, and fluid properties. The results will provide valuable guidelines for the optimal design and operation of double-pipe HEs in various applications, contributing to enhanced thermal efficiency and energy savings in industries relying on heat exchange processes. Therefore, this study provides a detailed computational investigation into the impact of varying pipe lengths on 2D heat exchanger performance, as follows:

- It focuses on the relationship between pipe length and key parameters such as heat exchanger efficiency and LMTD.
- Our study uniquely explores how pipe length affects heat transfer effectiveness in both parallel and counterflow systems.
- It offers a clear, quantifiable comparison of heat transfer performance across different pipe length.

## 2- Methods

### 2-1-Heat Exchanger Performance Analysis Using Log Mean Temperature Difference (LMTD)

To design the heat exchanger and predict its performance, the inlet and outlet temperatures of the fluids, the total heat transfer coefficient, and the total surface area of heat transfer between fluids must be interconnected. Two of these relationships can be derived by applying the principal equilibrium of total energy to both the cold and hot liquids as shown in Figure 1 [13, 58].

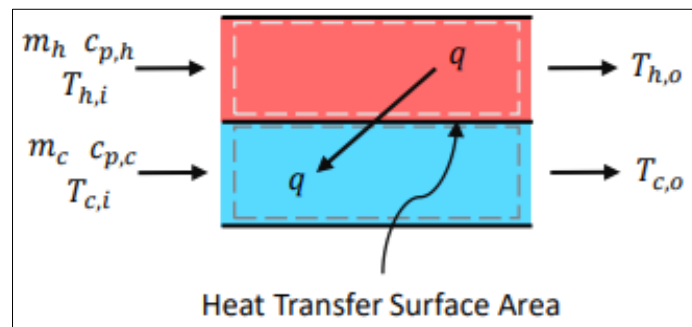


Figure 1. Energy balance between the inlet and outlet of a two-fluid [13]

When applying the equations of steady flow energy to the process of heat transfer between the cold and hot fluids at the entrance and exit of the heat exchanger, the total heat transfer is represented by the following equations [13, 58]:

$$q = \dot{m}_h C_{p,h} (T_{h,i} - T_{h,o}) \quad (1-a)$$

$$q = \dot{m}_c C_{p,c} (T_{c,o} - T_{c,i}) \quad (1-b)$$

Finally, the overall heat transfer can be summarized by Equation 2, which relates the cold fluid to the hot fluid according to the overall heat exchange coefficient [58].

$$q = UA\Delta T_m \quad (2)$$

where  $\Delta T_m$  is the appropriate mean temperature difference and the values of the overall heat transfer coefficients can be extracted as a limited value based on the fluid type. Figure 2 makes it evident that the construction of the HE has a significant influence on the total heat exchange for the parallel and counter HE, which is based on the temperature difference as the log mean difference. The HE's structure affects heat transfer because the flow's direction affects the amount of heat transferred at each stage. As a component of the structure, the exchanger's length affects both the quantity of heat transfer and its duration, which can be changed.

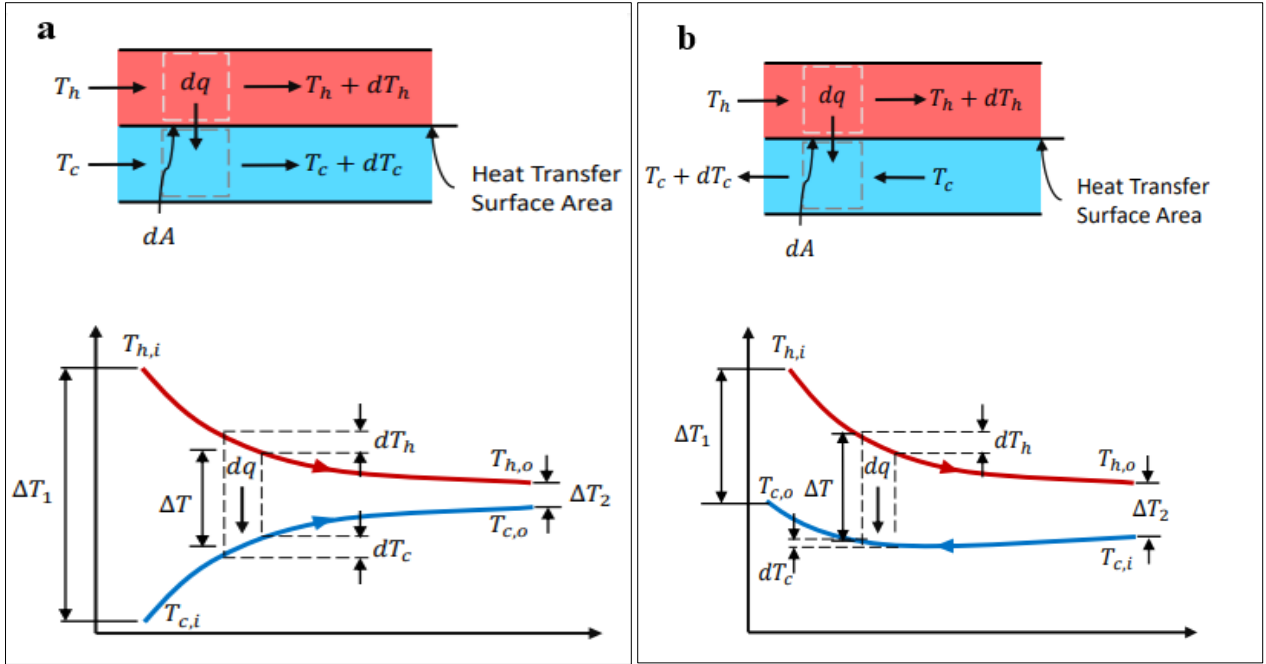


**Figure 2. (a) Temperature distribution for a parallel flow heat exchanger; (b) Temperature distribution for a counterflow heat exchanger**

Based on the HE's structure, the log mean temperature is determined under the assumptions of negligible axial conduction along the tube, and that the total heat transfer coefficient is constant. Thus, the log mean temperature difference can be expressed as follows:

$$\Delta T_{lm} = \frac{\Delta T_2 - \Delta T_1}{\ln\left(\frac{\Delta T_2}{\Delta T_1}\right)} \quad (3)$$

For parallel flow, it flows that  $T_{h,i} = T_{h,1}$ ,  $T_{h,o} = T_{h,2}$ ,  $T_{c,i} = T_{c,1}$ ,  $T_{c,o} = T_{c,2}$ , and therefore:  $\Delta T_1 = (T_{h,i} - T_{c,i})$ ;  $\Delta T_2 = (T_{h,o} - T_{c,o})$ .

For counter flow, it flows that  $T_{h,i} = T_{h,1}$ ,  $T_{h,o} = T_{h,2}$ ,  $T_{c,i} = T_{c,2}$ ,  $T_{c,o} = T_{c,1}$ , and therefore  $\Delta T_1 = (T_{h,i} - T_{c,o})$ ;  $\Delta T_2 = (T_{h,o} - T_{c,i})$ .

The effectiveness  $\varepsilon$  of a heat exchanger can be determined by the ratio of actual heat transfer in a heat exchanger to the maximum heat transfer that can be achieved by the heat exchanger.

$$\varepsilon = \frac{q}{q_{max}} \quad (4)$$

The maximum possible rate of heat transfer ( $q_{max}$ ) is achieved by the fluid with a minimum value of heat capacity ratio encountering the maximum  $\Delta T$  through the heat exchanger.

$$q_{max} = (\dot{m}C_p)_{min} \Delta T_{max} \quad (5)$$

where  $(\dot{m}C_p)_{min}$  is the minimum value of heat capacity rate that is equal to  $(\dot{m}C_p)_c$  or  $(\dot{m}C_p)_h$ , whichever is smaller, and  $\Delta T_{max}$  is equal to the temperature difference between hot and cold fluid at the inlet of heat exchanger ( $T_{h,i} - T_{c,i}$ ).

## 2-2-The CFD Methodology

The research approach is centered on evaluating the effects of HE pipes lengths ranging from 250, 550, 700, and 1000 mm using a CFD modeling program in order to identify the most suitable HE with the ideal length for different engineering applications. A comparison is then made between the effects of the various lengths of the work on the thermal effectiveness of HE, then completing the comparison by testing the subsequent length. The CFD analysis methodology is shown in Figure 3.

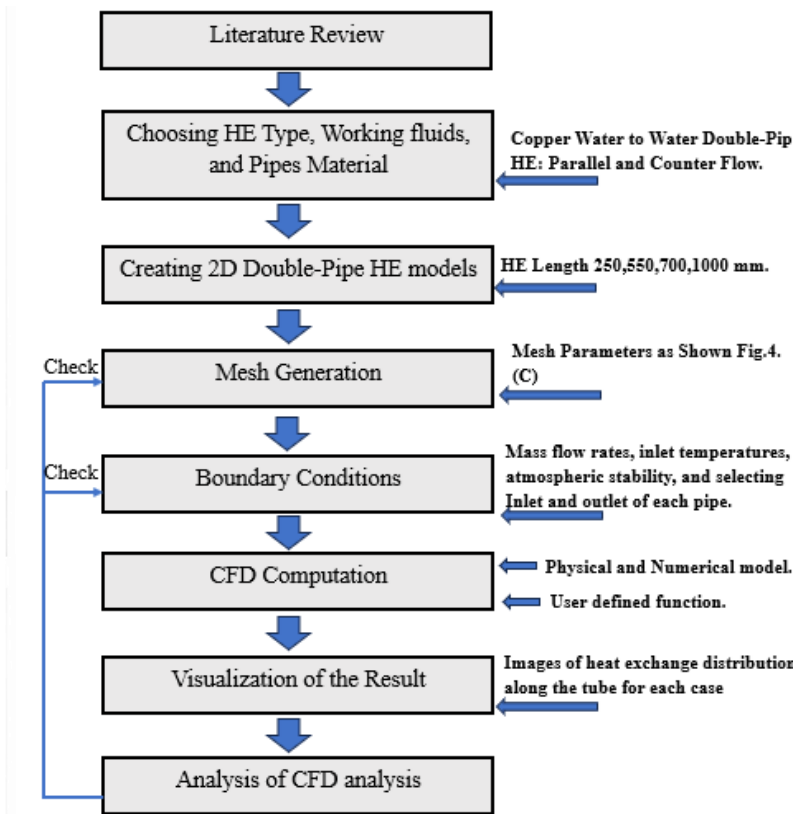


Figure 3. The CFD Methodology

2-2-1- Geometry Modeling

The two-dimensional HE geometry is built in the ANSYS workbench design module. It consists of an outer tube of copper with a 32.45 mm diameter, inside which there is another copper tube with a 25.4 mm diameter.

2-2-2- Mesh Generation

The HE was created as a fine mesh of elements (rectangle-shaped elements) with a general size of 0.5 mm. In order to determine the number of elements, it has relied on the convergence of simulation results represented by the temperature difference between the inlet and outlet of cold and hot fluids. Figure 4 shows the HE meshes details. In order to determine the number of elements, it has relied on the convergence of simulation results represented by the temperature difference between the inlet and outlet of cold and hot fluids.

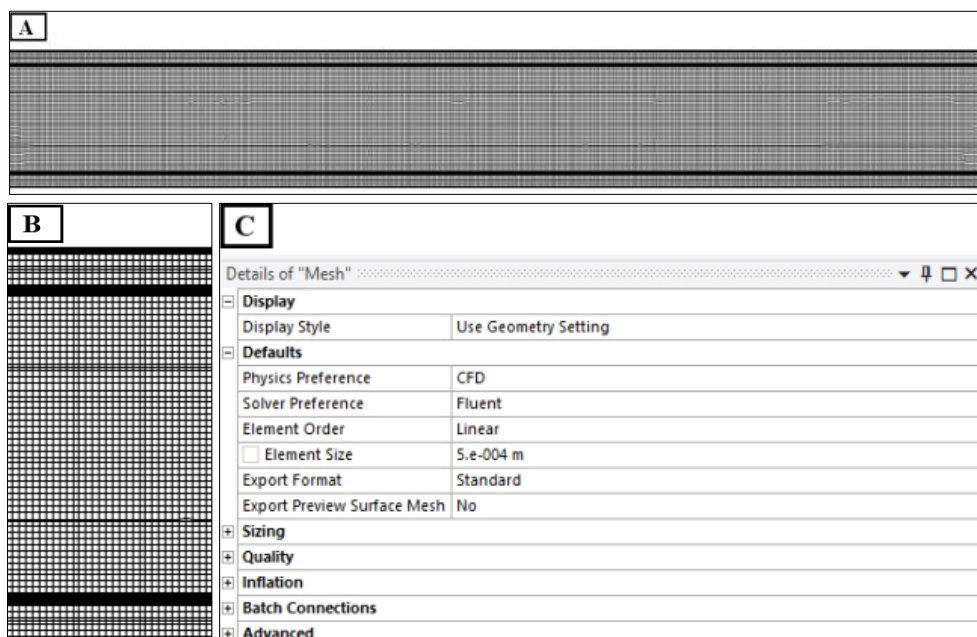


Figure 4. (A) Mesh Created; (B) Zoomed View; (C) Details of Mesh

### 2-2-3- Boundary Conditions

Boundary conditions include the definition of input conditions for inward and outward flow as indicated in Table 1. The output conditions of the inner flow and the outer flow are represented by the ambient condition.

**Table 1. Inlet boundary condition**

Inlet Conditions			
Inner Flow (Hot Fluid)		Outer Flow (Cold Fluid)	
Mass flow rate (Kg/s)	0.085	Mass flow rate (Kg/s)	0.085
Temperature (K)	328.15	Temperature (K)	299.15

### 3- Results and Discussion

The effects of HEs length were analyzed for different types, such as parallel and counterflow double-pipe HE. For a variety of system lengths involved, including 250, 550, 700, and 1000 mm, the effect of HEs length was examined. Figures 5-a to 5-d illustrate the temperature distribution between the hot and cold substances inside the parallel HE. The dark blue color indicates the lowest temperature, 299.15K, and the dark red color indicates the highest temperature, 328.15K.

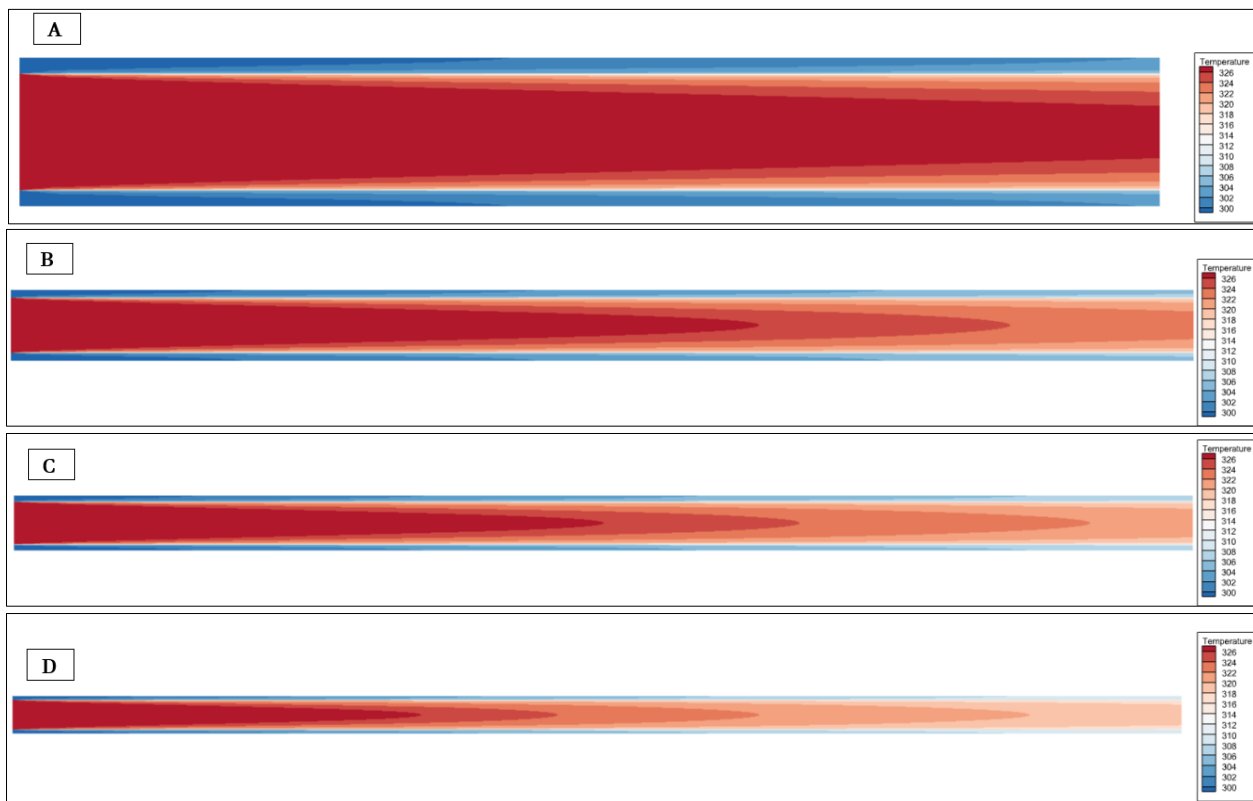


**Figure 5. Parallel HE temperature distribution at lengths of (A) 250 mm, (B) 550 mm, (C) 700 mm, and (D) 1000 mm**

The average temperature values at the cold and hot inlets and outlets of the parallel heat exchanger are shown in Table 2. Based on the simulation results, it is clear that the calculated log mean temperature difference of HE shrinks with increasing length, because the temperature difference between the hot and cold fluids becomes more uniform and smaller over a longer distance, and the logarithmic formula for LMTD reflects this reduction in temperature gradient, as shown in Figures 6-a to 6-d. It was 24.41 K for 250 mm, 20.79 K for 550 mm, 19.24 K for 700 mm, and 16.59 K for 1000 mm.

**Table 2. CFD Analysis Reading for Temperatures of Parallel HEs**

Heat Exchanger Length	Cold water temperature at the inlet	Hot water temperature at the inlet	Cold water temperature at the outlet	Hot water temperature at the outlet
250 mm	299.15 K	328.15 K	303.08 K	323.41 K
550 mm	299.15 K	328.15 K	306.26 K	320.56 K
700 mm	299.15 K	328.15 K	307.47 K	319.43 K
1000 mm	299.15 K	328.15 K	309.33 K	317.69 K

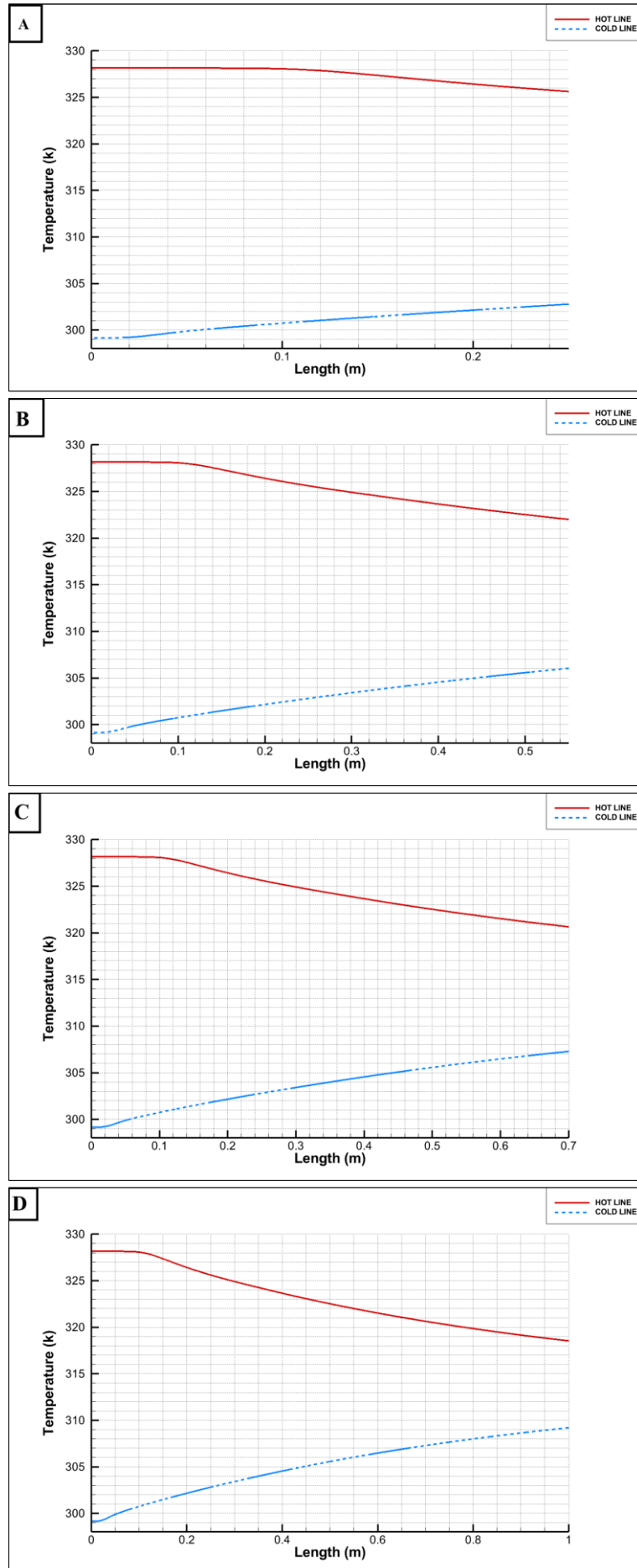


Figure 6. Temperature difference gap  $p$  in the parallel HE at lengths of (A) 250 mm, (B) 550 mm, (C) 700 mm, and (D) 1000 mm



Figure 7 shows how the effectiveness of the parallel-flow heat exchanger calculated based on the simulation results increases with increasing length, as it was 13.8% for 250 mm, 23.6% for 550 mm, 27.67% for 700 mm, and 33.98% for 1000 mm. This is due to the increase in the heat exchange surface area and the increase in the heat exchange duration, thus increasing the heat transfer rate. The results also show that the rate of improvement in HE's efficiency becomes noticeable with increasing length because a longer heat exchanger provides more surface area for heat transfer. As the length increases, the fluid has more time to interact with the surface, allowing more heat to be transferred between the hot and cold fluids. Additionally, longer heat exchangers can help improve the temperature difference between the fluids, which increases the overall effectiveness of the heat exchange process, which is what was supported in this study by Meesala et al. [57]. This leads to a more efficient system as heat transfer continues to improve with greater length.

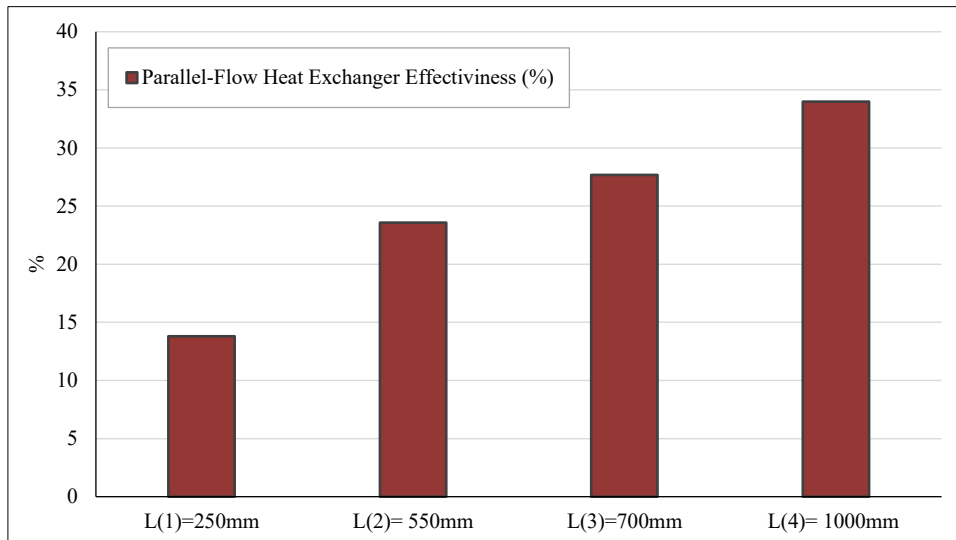


Figure 7. The parallel heat exchanger effectiveness

The internal temperature distribution of the counter-flow HE is shown in Figures 8-a to 8-d. The average temperature values at the cold and hot inlets and outlets of the counter heat exchanger are shown in Table 3. As the length of the HE increases, it is obvious that the log mean temperature difference of the HE shrinks, as shown in Figures 9-a to 9-d; it was 24.41 K for 250 mm, 21.156 K for 550 mm, 19.80 K for 700 mm, and 17.56 K for 1000 mm. When comparing the results for parallel flow and counterflow across the four different lengths, the logarithmic temperature value for counterflow is consistently higher than that for parallel flow. This difference becomes more pronounced as the length increases, because the counterflow HE maintains a more consistent and effective heat exchange due to the opposite flow directions, which is what was supported in this study [27].

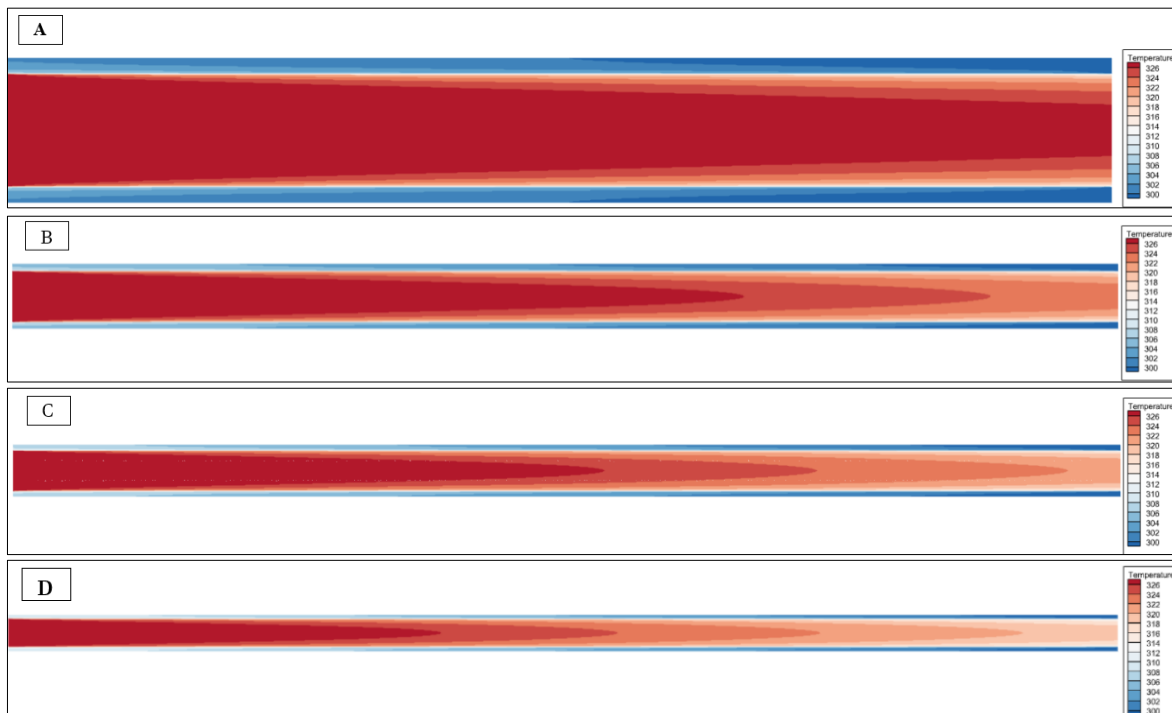
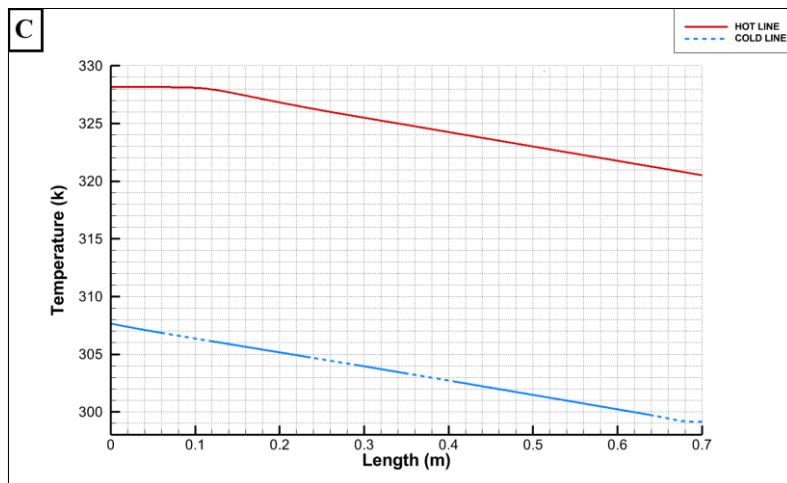
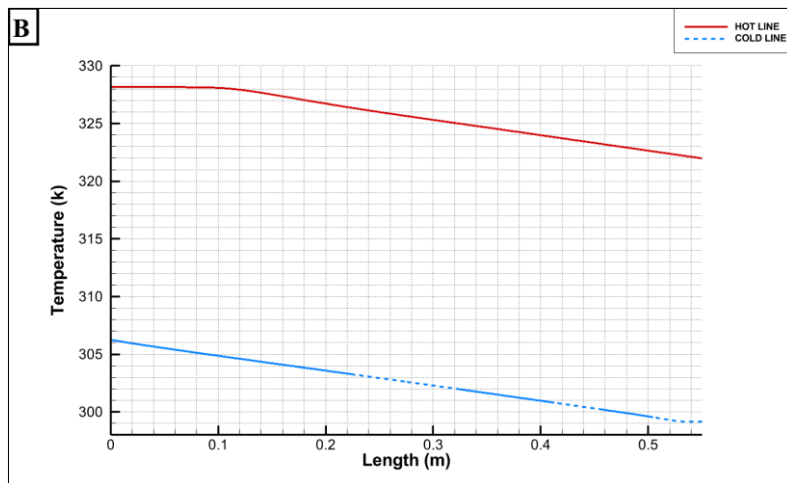
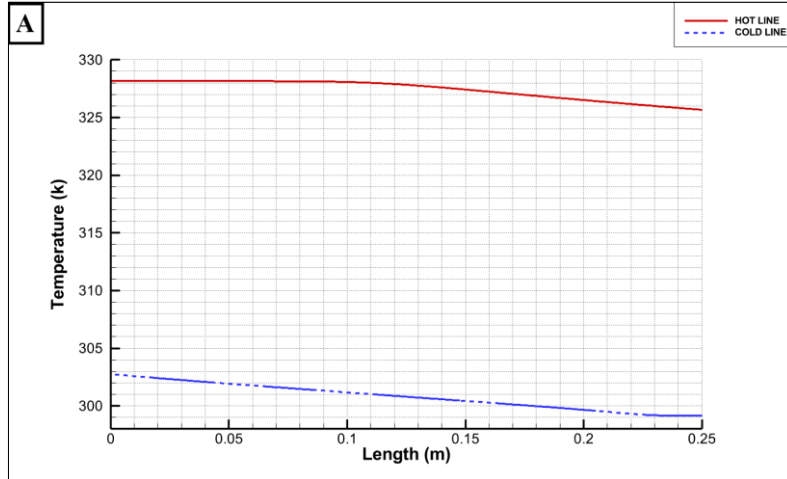


Figure 8. Counter HE temperature distribution at lengths of (A) 250 mm, (B) 550 mm, (C) 700 mm, and (D) 1000 mm



**Table 3. CFD Analysis Reading for Temperatures of Counter HEs**

Heat Exchanger Length	Cold water temperature at the inlet	Hot water temperature at the inlet	Cold water temperature at the outlet	Hot water temperature at the outlet
250 mm	299.15 K	328.15 K	303.27 K	323.16 K
550 mm	299.15 K	328.15 K	306.67 K	319.99 K
700 mm	299.15 K	328.15 K	308.04 K	318.65 K
1000 mm	299.15 K	328.15 K	310.33K	316.45 K



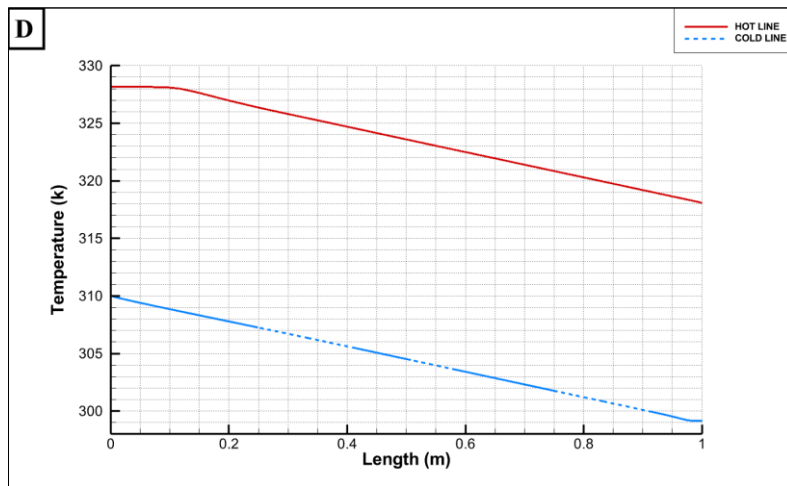


Figure 9. Temperature difference gap  $p$  in the counter HE at lengths of (A) 250 mm, (B) 550 mm, (C) 700 mm, and (D) 1000 mm

Improved counter-flow HE effectiveness calculated based on the simulation results is shown in Figure 10. The effectiveness was found to rise with the length of the HE, reaching 13.56% at 250 mm, 24.63% at 550 mm, 29.26% at 700 mm, and 36.95% inside the 1000 mm length HE.

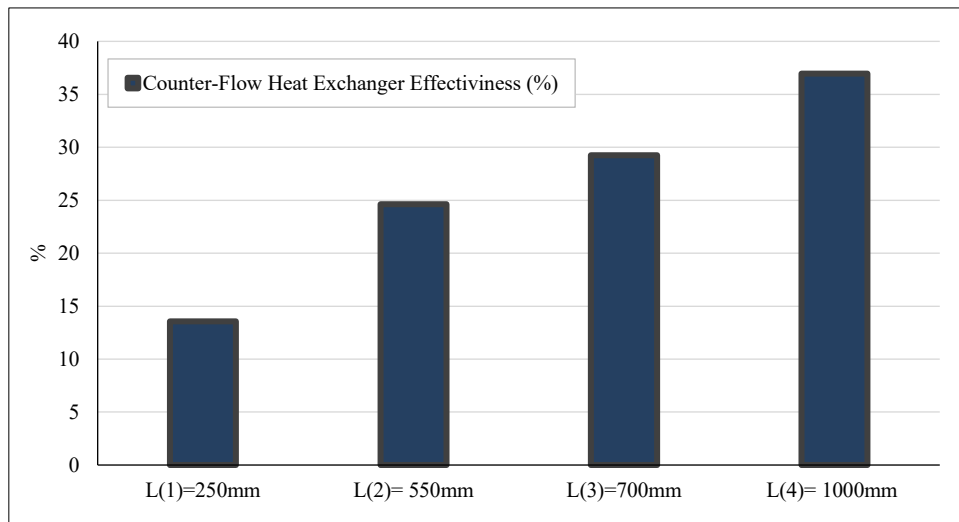


Figure 10. The counter heat exchanger effectiveness

A comparison between parallel and counterflow HEs showed that the effectiveness of counterflow becomes more evident compared to parallel flow, where the temperature gradient decreases with length, as shown in Figure 11.

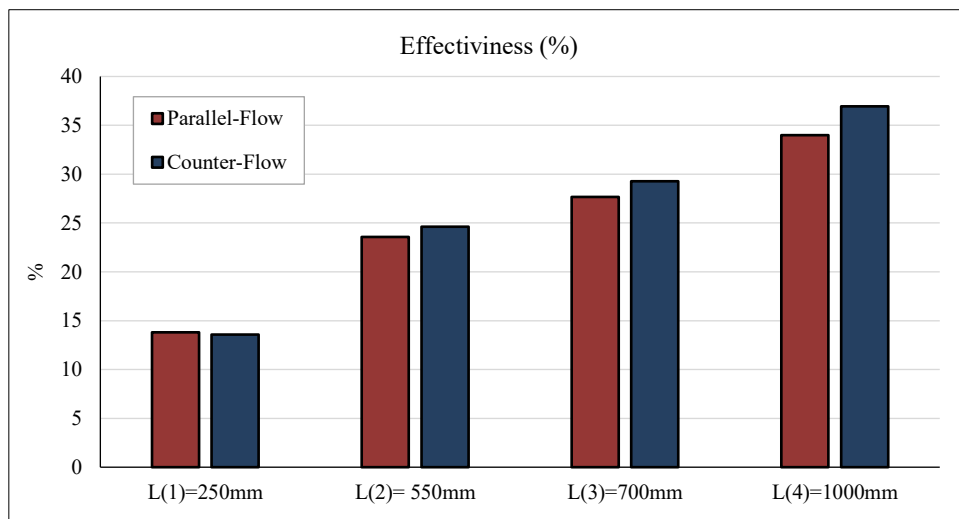


Figure 11. Effectiveness comparison between parallel and counter flow HEs

The results demonstrate how the design conditions impact the performance of heat exchangers (HEs). It was observed that the length of the HE significantly affects the heat exchange between the hot and cold materials. As the length increases, the heat exchange efficiency improves in both types of HEs, namely the parallel-flow and counter-flow exchangers. This improvement is attributed to the greater surface area for heat transfer and the extended exposure time for heat transfer between the materials. Additionally, the results indicate that the counter-flow HE is more efficient than the parallel-flow HE due to the larger temperature difference in the counter-flow exchanger.

Modern science has focused on improving the performance of heat exchangers (HEs) through several methods. Here we found Chang & Gwak [38] an increase in heat exchange surface area enhances heat transfer, which this study's findings supported. Alrwashdeh et al. [30] additionally examined the HE channels' length and discovered that internal HE design modifications increase the HE's efficiency. This conclusion aligns with the findings of this study, despite differences in analytical methods.

## 4- Conclusion

The results show that as the length of a heat exchanger increases, the temperature distribution becomes more uniform, leading to improved heat exchange efficiency. This improvement is attributed to the larger surface area and longer duration for heat transfer. Counter-flow heat exchangers are found to be more efficient than parallel-flow ones because they maintain a higher log mean temperature difference, which enhances heat transfer. Additionally, advancements in heat exchanger design, such as the optimization of fluid flow channels, have been shown to further improve heat exchange efficiency, as supported by previous studies.

## 5- Nomenclature

HE	Heat Exchanger	CFD	Computational Fluid Dynamics
$\Delta T_{LM}$ (LMTD)	Log Mean Temperature Difference, K	q	Heat transfer rate, W
$\dot{m}_c$	Mass flow rate, cold side, kg/s	$\dot{m}_h$	Mass flow rate, hot side, kg/s
$T_{h,i}, T_{h,o}$	Inner and outer hot temperatures, K	$T_{c,i}, T_{c,o}$	Inner and outer cold temperatures, K
A	Area, m <sup>2</sup>	$\Delta T_m$	Mean temperature differences, K
$C_{p,h}$	Specific heat at constant pressure, hot side, J/kg.K	$C_{p,c}$	Specific heat at constant pressure, cold side, J/kg.K.
$\epsilon$	The effectiveness.	U	Overall heat transfer coefficient, W/m <sup>2</sup> .K

## 6- Declarations

### 6-1-Data Availability Statement

The data presented in this study are available on request from the corresponding author.

### 6-2-Funding and Acknowledgements

This research is supported by Al-Balqa Applied University, Aqaba, Jordan, through the scientific research support program.

### 6-3-Institutional Review Board Statement

Not applicable.

### 6-4-Informed Consent Statement

Not applicable.

### 6-5-Conflicts of Interest

The author declares that there is no conflict of interest regarding the publication of this manuscript. In addition, the ethical issues, including plagiarism, informed consent, misconduct, data fabrication and/or falsification, double publication and/or submission, and redundancies have been completely observed by the author.

## 7- References

- [1] Omer, A. M. (2008). Energy, environment and sustainable development. *Renewable and Sustainable Energy Reviews*, 12(9), 2265–2300. doi:10.1016/j.rser.2007.05.001.
- [2] Armaroli, N., & Balzani, V. (2007). The future of energy supply: Challenges and opportunities. *Angewandte Chemie - International Edition*, 46(1–2), 52–66. doi:10.1002/anie.200602373.

- [3] Popp, D., Newell, R. G., & Jaffe, A. B. (2010). *Energy, the Environment, and Technological Change. Handbook of the Economics of Innovation*, Volume 2, 873–937, Elsevier, Amsterdam, Netherlands. doi:10.1016/s0169-7218(10)02005-8.
- [4] Asif, M., & Muneer, T. (2007). Energy supply, its demand and security issues for developed and emerging economies. *Renewable and Sustainable Energy Reviews*, 11(7), 1388–1413. doi:10.1016/j.rser.2005.12.004.
- [5] Hadjipaschalis, I., Poullikkas, A., & Efthimiou, V. (2009). Overview of current and future energy storage technologies for electric power applications. *Renewable and Sustainable Energy Reviews*, 13(6–7), 1513–1522. doi:10.1016/j.rser.2008.09.028.
- [6] Zohuri, B. (2016). *Application of Compact Heat Exchangers for Combined Cycle Driven Efficiency in Next Generation Nuclear Power Plants*. Springer International Publishing, Cham, Switzerland. doi:10.1007/978-3-319-23537-0.
- [7] Hajatzadeh Pordanjani, A., Aghakhani, S., Afrand, M., Mahmoudi, B., Mahian, O., & Wongwises, S. (2019). An updated review on application of nanofluids in heat exchangers for saving energy. *Energy Conversion and Management*, 198, 111886. doi:10.1016/j.enconman.2019.111886.
- [8] Shabgard, H., Allen, M. J., Sharifi, N., Benn, S. P., Faghri, A., & Bergman, T. L. (2015). Heat pipe heat exchangers and heat sinks: Opportunities, challenges, applications, analysis, and state of the art. *International Journal of Heat and Mass Transfer*, 89, 138–158. doi:10.1016/j.ijheatmasstransfer.2015.05.020.
- [9] Hesselgreaves, J. E., Law, R., & Reay, D. (2016). *Compact heat exchangers: selection, design and operation*. Butterworth-Heinemann, Oxford, United Kingdom. doi:10.1016/B978-0-08-100305-3.00008-2.
- [10] McDonald, C. F. (1989). The increasing role of heat exchangers in gas turbine plants. Vol. 79160, V004T09A005, American Society of Mechanical Engineers, New York, United States. doi:10.1115/89-GT-103.
- [11] Mills, A. F. (1992). *Heat transfer*. CRC Press, Routledge, New York, United States. doi:10.4324/9780203752173.
- [12] Kaviany, M. (2012). *Principles of heat transfer in porous media*. Springer Science & Business Media, New York, United States. doi:10.1007/978-1-4612-4254-3.
- [13] Sekulić, D. P., & Sha, R. K. (2023). *Fundamentals of heat exchanger design*. John Wiley & Sons, Hoboken, United States. doi:10.1002/9781119883296.
- [14] Shah, R. K., & Sekulic, D. P. (1998). *Heat exchangers* John Wiley & Sons, Hoboken, United States.
- [15] Fraas, A. P. (1991). *Heat exchanger design*. John Wiley & Sons, Hoboken, United States.
- [16] Vekariyamukesh, V., Selokar, G. R., & Paul, A. (2012). Optimization and Design of Heat Exchanger with Different Materials. *International Journal of Mathematical Engineering and Management Sciences*, 5(1), 37–42.
- [17] Marzouk, S. A., Abou Al-Sood, M. M., El-Said, E. M. S., Younes, M. M., & El-Fakharany, M. K. (2023). A comprehensive review of methods of heat transfer enhancement in shell and tube heat exchangers. *Journal of Thermal Analysis and Calorimetry*, 148(15), 7539–7578. doi:10.1007/s10973-023-12265-3.
- [18] Amor, N., Adach, K., Noman, M. T., Hazuka, F., & Fijalkowski, M. (2024). Advances in heat exchangers for heat and mass transfer: a review. *Journal of the Textile Institute*, 115(12), 2678–2692. doi:10.1080/00405000.2024.2311226.
- [19] Agarwal, P., Adhirathsik, & Shanthi, V. (2014). Application of heat exchangers in bioprocess industry: A review. *International Journal of Pharmacy and Pharmaceutical Sciences*, 6(1), 24–28.
- [20] Adam, A. Y., Oumer, A. N., Najafi, G., Ishak, M., Firdaus, M., & Aklilu, T. B. (2019). State of the art on flow and heat transfer performance of compact fin-and-tube heat exchangers. *Journal of Thermal Analysis and Calorimetry*, 139(4), 2739–2768. doi:10.1007/s10973-019-08971-6.
- [21] Kays, W.M. and London, A.L. (1984) *Compact Heat Exchangers* (3<sup>rd</sup> Ed.). McGraw-Hill Book Company, Columbus, United States.
- [22] Gude, V. G. (2015). Energy storage for desalination processes powered by renewable energy and waste heat sources. *Applied Energy*, 137, 877–898. doi:10.1016/j.apenergy.2014.06.061.
- [23] Lee, H. (2022). *Thermal Design: Heat Sinks, Thermoelectrics, Heat Pipes, Compact Heat Exchangers, and Solar Cells* (2<sup>nd</sup> Ed.). John Wiley & Sons, Hoboken, United States. doi:10.1002/9781119686040.
- [24] Karwa, R. (2020). Heat Exchangers. In: *Heat and Mass Transfer*. Springer, Singapore. doi:10.1007/978-981-15-3988-6\_14.
- [25] Pacio, J. C., & Dorao, C. A. (2011). A review on heat exchanger thermal hydraulic models for cryogenic applications. *Cryogenics*, 51(7), 366–379. doi:10.1016/j.cryogenics.2011.04.005.
- [26] Miguel, A. F., & Rocha, L. A. O. (2018). *Tree-Shaped Fluid Flow and Heat Transfer*. Springer International Publishing, Cham, Switzerland. doi:10.1007/978-3-319-73260-2.
- [27] Chen, K., & Gwilliam, S. B. (1996). An analysis of the heat transfer rate and efficiency of TE (thermoelectric) cooling systems. *International Journal of Energy Research*, 20(5), 399–417. doi:10.1002/(SICI)1099-114X(199605)20:5<399::AID-ER160>3.0.CO;2-R.

- [28] Zhang, H. L., & Davie, C. T. (2013). A numerical investigation of the influence of pore pressures and thermally induced stresses for spalling of concrete exposed to elevated temperatures. *Fire Safety Journal*, 59, 102–110. doi:10.1016/j.firesaf.2013.03.019.
- [29] Mangrulkar, C. K., Dhoble, A. S., Pant, P. K., Kumar, N., Gupta, A., & Chamoli, S. (2020). Thermal performance escalation of cross flow heat exchanger using in-line elliptical tubes. *Experimental Heat Transfer*, 33(7), 587–612. doi:10.1080/08916152.2019.1704946.
- [30] Alrwashdeh, S. S., Ammari, H., Madanat, M. A., & Al-Falahat, A. M. (2022). The Effect of Heat Exchanger Design on Heat transfer Rate and Temperature Distribution. *Emerging Science Journal*, 6(1), 128–137. doi:10.28991/ESJ-2022-06-01-010.
- [31] Sahin, B., Yakut, K., Kotcioglu, I., & Celik, C. (2005). Optimum design parameters of a heat exchanger. *Applied Energy*, 82(1), 90–106. doi:10.1016/j.apenergy.2004.10.002.
- [32] Ghaderi, A., Veysi, F., Aminian, S., Andami, Z., & Najafi, M. (2022). Experimental and Numerical Study of Thermal Efficiency of Helically Coiled Tube Heat Exchanger Using Ethylene Glycol-Distilled Water Based Fe<sub>3</sub>O<sub>4</sub> Nanofluid. *International Journal of Thermophysics*, 43(8), 118. doi:10.1007/s10765-022-03041-w.
- [33] Ajay, K., Kumar, R., Gupta, A., Gokahale, O., & Mukhopadhyay, D. (2023). Understanding the influence of eccentric pressure tube on the thermal behavior of 37-element based PHWR channel under accident condition. *Annals of Nuclear Energy*, 181, 109533. doi:10.1016/j.anucene.2022.109533.
- [34] Khaled, A. R. A., Siddique, M., Abdulhafiz, N. I., & Boukhary, A. Y. (2010). Recent advances in heat transfer enhancements: A review report. *International Journal of Chemical Engineering*, 1, 106461. doi:10.1155/2010/106461.
- [35] Xie, X., Chen, Y., Dai, L., & Xu, L. (2024). Modeling and experimental study of air-cooled finned-tube condenser using coupled distribution parameter method and air-side temperature distribution. *Applied Thermal Engineering*, 249, 123411. doi:10.1016/j.applthermaleng.2024.123411.
- [36] Zhao, L., & Deng, J. (2023). Numerical study on the heat transfer enhancement outside the pipe bundle under the effect of continuous pressure waves. *International Journal of Heat and Mass Transfer*, 207, 123994. doi:10.1016/j.ijheatmasstransfer.2023.123994.
- [37] Bhattacharyya, S., Vishwakarma, D. K., Srinivasan, A., Soni, M. K., Goel, V., Sharifpur, M., Ahmadi, M. H., Issakhov, A., & Meyer, J. (2022). Thermal performance enhancement in heat exchangers using active and passive techniques: a detailed review. *Journal of Thermal Analysis and Calorimetry*, 147(17), 9229–9281. doi:10.1007/s10973-021-11168-5.
- [38] Chang, H. M., & Gwak, K. H. (2015). New application of plate-fin heat exchanger with regenerative cryocoolers. *Cryogenics*, 70, 1–8. doi:10.1016/j.cryogenics.2015.04.005.
- [39] Kirsch, K. L., & Thole, K. A. (2017). Pressure loss and heat transfer performance for additively and conventionally manufactured pin fin arrays. *International Journal of Heat and Mass Transfer*, 108, 2502–2513. doi:10.1016/j.ijheatmasstransfer.2017.01.095.
- [40] Maji, A., Bhanja, D., & Patowari, P. K. (2019). Computational investigation and optimisation study on system performance of heat sink using perforated pin fins mounted at different angles. *Progress in Computational Fluid Dynamics*, 19(6), 381–400. doi:10.1504/pcfd.2019.10024493.
- [41] Effendi, N. S., & Kim, K. J. (2018). Natural convective hybrid fin heat sinks for lightweight and high performance thermal management. *Journal of Mechanical Science and Technology*, 32(10), 5005–5013. doi:10.1007/s12206-018-0948-4.
- [42] Guo, Z. Y., & Li, Z. X. (2003). Size effect on microscale single-phase flow and heat transfer. *International Journal of Heat and Mass Transfer*, 46(1), 149–159. doi:10.1016/S0017-9310(02)00209-0.
- [43] Jiang, P.-X., Fan, M.-H., Si, G.-S., & Ren, Z.-P. (n.d.). Thermal-hydraulic performance of small-scale micro-channel and porous-media heat exchangers. *International Journal of Heat and Mass Transfer*, 44(5), 1039–1051.
- [44] Siddiqui, O. K., & Zubair, S. M. (2017). Efficient energy utilization through proper design of microchannel heat exchanger manifolds: A comprehensive review. *Renewable and Sustainable Energy Reviews*, 74, 969–1002. doi:10.1016/j.rser.2017.01.074.
- [45] Abar, S., Theodoropoulos, G. K., Lemarinier, P., & O'Hare, G. M. P. (2017). Agent Based Modelling and Simulation tools: A review of the state-of-art software. *Computer Science Review*, 24, 13–33. doi:10.1016/j.cosrev.2017.03.001.
- [46] Tu, J., Yeoh, G. H., Liu, C., & Tao, Y. (2024). *Computational Fluid Dynamics: A Practical Approach*. Butterworth-Heinemann, Oxford, United Kingdom. doi:10.1016/C2021-0-01771-5.
- [47] Oyewola, O. M., Awonusi, A. A., & Ismail, O. S. (2024). Performance Optimization of Step-Like Divergence Plenum Air-Cooled Li-Ion Battery Thermal Management System Using Variable-Step-Height Configuration. *Emerging Science Journal*, 8(3), 795–814. doi:10.28991/ESJ-2024-08-03-01.
- [48] Anderson, D., Tannehill, J. C., Pletcher, R. H., Munipalli, R., & Shankar, V. (2020). *Computational fluid mechanics and heat transfer*. CRC Press, Boca Raton, United States. doi:10.1201/9781351124027.

- [49] Wei, Y. (2017). The development and application of CFD technology in mechanical engineering. IOP Conference Series: Materials Science and Engineering, 274(1), 12012. doi:10.1088/1757-899X/274/1/012012.
- [50] Zikanov, O. (2019). Essential computational fluid dynamics. John Wiley & Sons, Hoboken, United States.
- [51] Ashgriz, N., & Mostaghimi, J. (2002). An introduction to computational fluid dynamics. Fluid Flow Handbook, 1-49.
- [52] Kuipers, J. A. M., & van Swaaij, W. P. M. (1997). Application of Computational Fluid Dynamics to Chemical Reaction Engineering. Reviews in Chemical Engineering, 13(3), 1–118. doi:10.1515/revce.1997.13.3.1.
- [53] Löhner, R. (2008). Applied Computational Fluid Dynamics Techniques. John Wiley & Sons, Hoboken, United States. doi:10.1002/9780470989746.
- [54] Kutler, P. (1985). A perspective of theoretical and applied computational fluid dynamics. AIAA Journal, 23(3), 328–341. doi:10.2514/3.8917.
- [55] Karwa, C. A. (2019). Finite element modelling and analysis of the friction stir extrusion process. Master Thesis, The Ohio State University, Columbus, United States.
- [56] Saha, C. K., Yi, Q., Janke, D., Hempel, S., Amon, B., & Amon, T. (2020). Opening size effects on airflow pattern and airflow rate of a naturally ventilated dairy building-A CFD study. Applied Sciences (Switzerland), 10(17), 6054. doi:10.3390/app10176054.
- [57] Meesala, S. K., Govinda Rao, B., & Yellapragada, D. B. (2023). Effect of pipe rotation on heat transfer to laminar non-Newtonian nanofluid flowing through a pipe: A CFD analysis. Chemical Product and Process Modeling, 18(3), 487–503. doi:10.1515/cppm-2022-0021.
- [58] Khayal, O. M. E. S. (2018). Fundamentals of heat exchangers. International Journal of Research in Comp. Applications and Robotics, 6(12), 1-11.